# Evolution of mechanical properties and corrosion resistance of Al-Zn-Mg alloy with different numbers of flame rectification at 350°C


## ABSTRACT

This paper investigated the microstructure, tensile properties, intergranular corrosion resistance and exfoliation corrosion resistance of Al-4.5Zn-1.5Mg (wt.%) alloy after undergoing different numbers of flame rectification at 350°C. The results showed that in the flame correction area, the mechanical properties of Al-4.5Zn-1.5Mg(wt.%) alloy with two times of flame correction is the best. The maximum tensile strength and elongation of Al-4.5Zn-1.5Mg(wt.%) alloy inside the region of flame correction are 387MPa and 26.37% respectively. The flame rectification accelerated the corrosion susceptibility of Al-4.5Zn-1.5Mg(wt.%) alloy. The maximum intergranular corrosion depth is detected with the value of 105μm after one time of FR. The corrosion property of Al-4.5Zn-1.5Mg(wt.%) alloy is mainly related to the formation of galvanic couple. The uneven distribution of the second phase particles of Al-4.5Zn-1.5Mg(wt.%) alloys results in different corrosion potentials at grain boundaries and within grains, leading to galvanic corrosion.



*Keywords: Al-Zn-Mg alloy; flame rectification; microstructure; mechanical properties; corrosion properties.*


## 1. INTRODUCTION

Al-Zn-Mg alloys are widely used because of their high specific strength, hardness, good weldability and corrosion resistance. However, the difficulty in controlling residual stress and deformation of Al-Zn-Mg alloys has become a major challenge. To solve this challenge, flame rectification (FR) is a great method [1]. Due to the uneven heating and cooling of the welding process, welding deformation of Al alloy workpieces is inevitable. Currently, there are three categories of measures available to control welding distortion: 1. Before welding, during the design stage of welding structure, welding deformations can be predicted using computational methods (such as numerical simulation techniques). Subsequently, measures such as optimizing structural design and positioning weld seams reasonably can be employed to "proactively" control welding deformations. 2. During welding, in the stage of welding manufacturing (assembly),"proactive" control of welding deformations can be achieved by controlling heat input, optimizing welding sequences, and utilizing external constraints and counter-deformation measures. 3. Post-weld heat treatment (thermal correction or mechanical correction), which falls under the category of "passive" control methods, which may increase costs and energy consumption [2,3]. If welding distortion cannot be controlled within the allowable range by using pre- welding and during-welding straightening methods, it is necessary to carry out post-welding correction.

The methods of post-weld straightening include mechanical straightening method (cold straightening) and FR method (heat straightening) [4,5]. Mechanical straightening is the use of mechanical methods such as hammering, presses and other mechanical methods to counteract welding distortion of structural components by inducing plastic deformation in the weld material. The FR is based on the characteristics of heat expands and cold contracts of metal materials. In the welding distortion area after heating and cooling, so that the welded structural components to produce anti-deformation, to achieve the purpose of correcting the welding distortion [6,7]. Mechanical straightening is generally suitable for small parts, and FR is mainly suitable for large structural parts. FR can be divided into spot heating, linear heating and triangle heating according to heating methods, as shown in Fig.1 [8]. Fig. 2 shows the schematic diagram of the principle of triangular FR [8].The FR is typically heated

by an oxygen-acetylene flame, with a maximum temperature of approximately 3200°C. By moving the oxyacetylene flame, the distortion area is heated and then quenching in water immediately, which in turn reduces the welding distortion. The FR is widely used in the production of straightening of welding distortion of structural parts of iron and steel materials due to the advantages of easy operation and flexibility [8,9]. With the continuous expansion of the application scope of high-strength Al alloy in the field of equipment manufacturing. The Al alloy FR process and its impact on the structure properties of components is gradually attracting extensive attention from researchers.

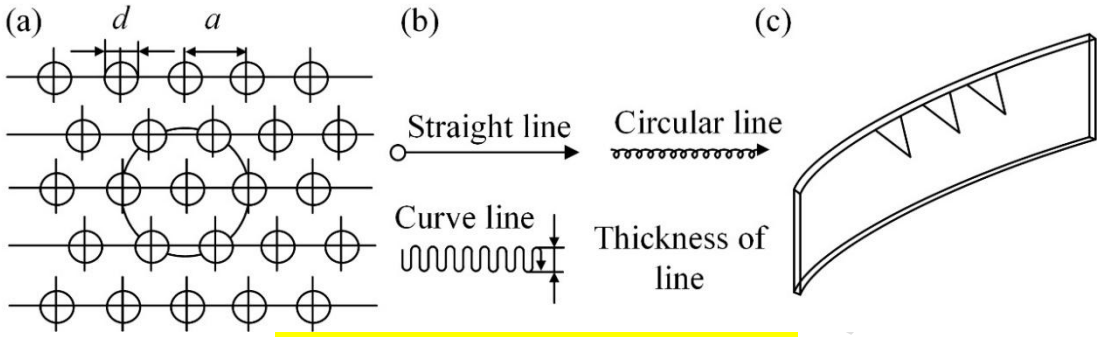


Fig. 1. The common heating methods for FR
(a) spot heating, (b)linear heating, and (c) triangle heating [8]

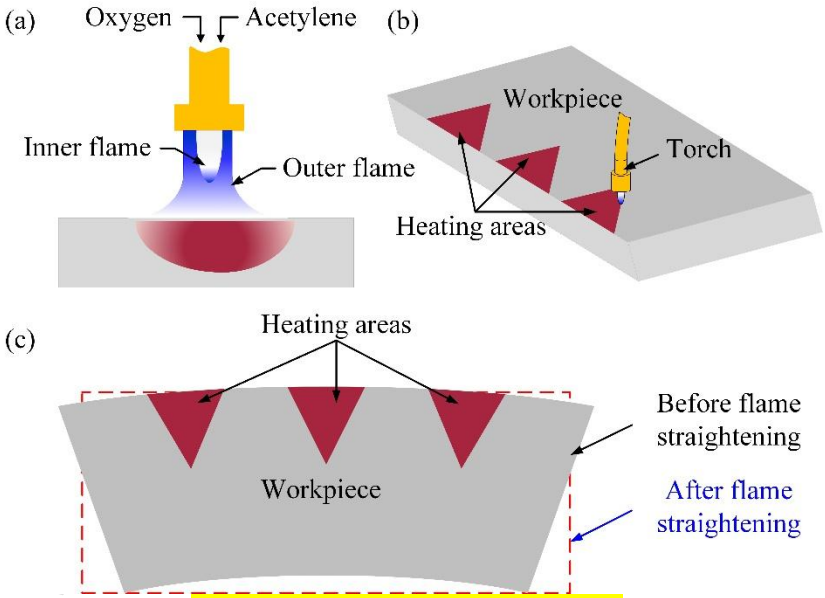


Fig. 2. The schematic diagram of FR
(a) FR, (b) heat areas, and (c) before and after FR [8]

Jiang [9] used flame heating to correct the welding distortion of 7020 Al alloy. The findings demonstrate that the mechanical properties of the welded joints remain unchanged at a correction temperature of 125°C. However, at temperatures above 225°C, there is a gradual increase in the tensile strength of the joints with an increase in correction temperature. Additionally, when the straightening temperature reaches above 325°C, the softening zone becomes wider, and the hardness reduces gradually with an increase in straightening temperature. Therefore, it is recommended that the correction of 7020 Al alloy should be carried out below 325°C. Temperature field tests have shown that FR creates an unstable instantaneous temperature field that is vulnerable to operational factors [10]. Moreover, Avent [11-13] stressed that "the process remains more of an art than a science". Thus, it is evident that the use of flame heating method cannot precisely analyze the causes

of the alteration in alloy performance. To better investigate the influence of heat treatment parameters on the microstructure and properties of 7N01 Al alloy. Xiong [10] conducted a study on the impact of FR temperature on the microstructure as well as mechanical properties of Al alloy joints in high-speed trains, using Gleeble thermal simulation testing machine. The study revealed that the FR temperature did not significantly alter the hardness of the weld zone. However, the hardness of the 7N01 Al alloy base metal and the heat-affected zone decreased when the temperature was below 300°C, whereas it increased between 300-350°C. Therefore, the recommended heat correction temperature for 7N01 Al alloy is between 300-400°C.

## 2. MATERIALS AND METHODS

### 2.1 MATERIALS AND FLAME CONDITIONING METHODS

The base material in this paper is Al-4.5Zn-1.5Mg-T5(wt.%) profile. The material size is 5mm×40mm×140mm. The chemical composition of base material is as shown in the Table 1.

Table 1 Chemical composition of Al-Zn-Mg alloy (wt.%)

| Materials | Zn | Mg | Mn | Cr | Zr | Fe | Cu | Ti | Si | Al |
|---|---|---|---|---|---|---|---|---|---|---|
| Al4.5Zn1.5Mg-T5 | 4.48 | 1.55 | 0.29 | 0.23 | 0.18 | 0.13 | 0.11 | 0.05 | 0.05 | Bal |

During the FR, combustible mixed gases, including oxygen-acetylene flame, are employed to heat the corrective area. The flame heating process generates a local transient temperature field, which varies with heating time and location. Furthermore, it is influenced by operational factors, can not obtain a stable temperature field, which hinders precise control of the corrective temperature. To better investigate the effects of FR parameters on the phase transformation and corrosion performance of Al-Zn-Mg alloy, reduce the influence of other factors on experimental results, and make the experimental conclusions more convincing. In this paper, the effect of FR on the mechanical and corrosion properties of Al-Zn-Mg alloys is investigated, and the FR process of Al-Zn-Mg-T5 alloy samples are shown in Table 2.

Table 2 The FR process of Al-Zn-Mg-T5 alloy samples

| Samples No. | Number of times in heat treatment | Temperature (°C) | Heating time (s) |
|---|---|---|---|
| BM | - | - | - |
| WQ1 | 1 | 350 | 120 |
| WQ2 | 2 | 350 | 120 |
| WQ3 | 3 | 350 | 120 |

### 2.2 MICROSTRUCTURE OBSERVATION AND ANALYSIS

The treated specimens were coarsely ground and finely ground to 2000 grit size with SiC sandpaper. Polishing with diamond abrasive paste with a grain size of 1.5 μm. After polishing was completed, the corrosion was carried out with mixed acid (2 mL HF + 3 mL HCl + 5 mL $HNO_3$ + 190 mL $H_2O$), and the corrosion time was about 45 s. Immediately after corrosion, rinse with clean water and dry with a hair dryer. The metallographic structure of Al-Zn-Mg alloy matrix was observed by Leica MEF4 metallographic microscope.

The microstructures of the alloys and welded joints were observed and analyzed using a Zeiss supra55 Field Emission Scanning Electron Microscope (SEM) with Energy Dispersive Spectroscopy (EDS). SEM second electron images were used to analyze fracture of room temperature tensile and slow strain rate tensile specimens under different heat treatment

conditions to determine the fracture mechanism. It can also be used to observe local corrosion morphology and compositional analysis.

The specimens were analyzed using the Electron Backscattered Diffraction (EBSD) analysis function attached to the SEM. EBSD samples underwent coarse grinding, fine grinding, and mechanical polishing, then they were subjected to electrolytic polishing to remove surface stress. The electrolyte solution consists of 30% nitric acid and 70% methanol (by volume at a temperature of -30°C. For electrolytic polishing, the voltage was set at 15 V, and the electrolytic polishing time ranged from 10 to 20 seconds. After electropolishing, the sample is cleaned in alcohol to remove residual corrosive liquid, then it is rins using an ultrasonic cleaning machine. Afterwards, sample is removed and dried with a hair dryer before further processing. For EBSD observation, the applied voltage is 20 kV, and the step size is 1.5 μm.

## 2.3 MECHANICAL PROPERTIES TEST AT ROOM TEMPERATURE

The tensile test samples at room temperature were prepared according to the standard GB/T 228.1-2010. The test equipment was DNS100 universal tensile testing machine, with a tensile rate of 5 mm/min, and each measured value was the average of three sets of parallel samples. The dimension used for the thermal cycling is as shown in Fig. 3.

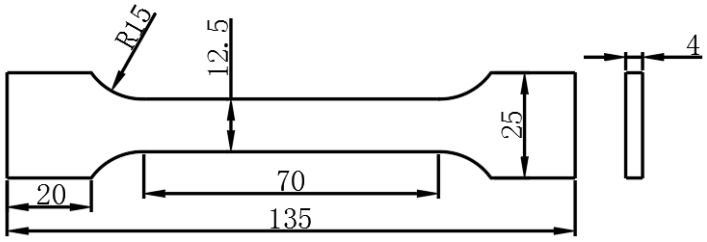


Fig. 3. Dimensions of repetitious FR samples for tensile test (Unit, mm)

## 2.4 CORROSION PERFORMANCE TEST

The intergranular corrosion test was conducted according to the standared ASTM G110-92 and the samples with dimensions of 40 mm× 25 mm× 5 mm were extracted from the samples after FR for intergranular corrosion (IGC) test [14]. Before the experiment, polish the samples with SiC sandpaper up to 1200 grit, and rinse them with acetone to remove surface oil contaminants. The sample was immersed in a 10 wt.% NaOH solution for 5-15 minutes, then removed and rinsed with deionized water. Subsequently placed in 30 vol.% $HNO_3$ solution until the surface of the specimen is bright. Rinse with deionized water and dry with a hair dryer .The non-working surface of the specimen was sealed with epoxy AB glue. The intergranular corrosion solution was composed of 57g of pure NaCl and 10mL of pure $H_2O_2$, which were diluted to 1L with deionized water. Maintain the soaking temperature within the range of 35±2 °C using a thermostatic water bath. After completing the intergranular corrosion test, the specimen was mechanically cut 5 mm from the specimen in the direction of the perpendicular main deformation. Then embed the sample for grinding and polishing, then use an optical microscope (OM) to observe and measure the corrosion depth.

The exfoliation corrosion (EXCO) test was conducted according to the standard ASTM G34-01 [15]. The specimens were prepared as follows: sandpaper sanding → acetone cleaning → deionized water cleaning → blow-drying. The corrosion solution composition is: 4 M NaCl + 0.5 M $KNO_3$ + 0.1 M $HNO_3$, the pH value of the solution is about 0.4, and the temperature of the corrosion solution is maintained at 25 ± 2 °C. The specimen is immersed in a corrosive solution and removed at regular intervals. The macroscopic corrosion morphology of the specimen surface was recorded with a camera, and the exfoliation corrosion grade was assessed with a total immersion time of 48 h.

## 3. EXPERIMENTAL RESULTS AND ANALYSIS

### 3.1 COMPARATIVE ANALYSIS OF MICROSTRUCTURE

The microstructure of Al-4.5Zn-1.5Mg (wt.%) alloy inside the region of flame rectification after different numbers of FR is shown in Fig. 4. It shows that the Al-4.5Zn-1.5Mg (wt.%) alloy consists of a large number of elongated grains distributed along the extrusion direction, and there is no obvious recrystallization. A large number of fine and diffuse MgZn2 precipitation phases are distributed both in the grain and at the grain boundaries. Compared with the unstraightened area, the number of intracrystalline precipitates was slightly reduced after the first 350°C-flame straightening, there was a tendency to dissolve into the matrix, and the grains grew significantly.

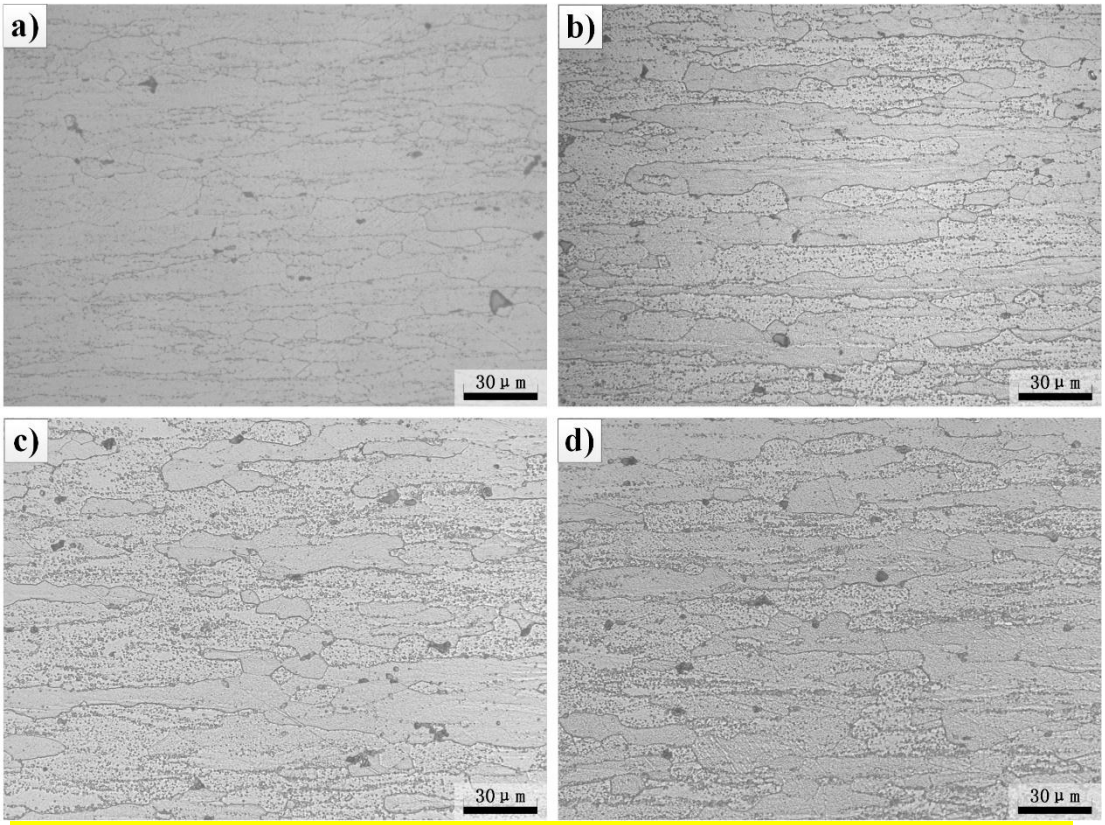


Fig. 4. Microstructure of Al-4.5Zn-1.5Mg (wt.%) alloy inside the region of flame rectification after different numbers of FR in 350°C
(a) base metal, (b) one time, (c) two times, and (d) three times

### 3.2 COMPARATIVE ANALYSIS OF MECHANICAL PROPERTIES

Fig. 5 shows the tensile strength and elongation of Al-4.5Zn-1.5Mg(wt.%) alloy inside the area of flame rectification in 350°C. It can be observed that after a single FR at 350°C, the tensile strength of the alloy significantly decreases to 317MPa. However, after the second and third FR, the strength rise again and noticeably higher than the value before straightening. The trend of elongation was similar to that of tensile strength. The maximum tensile strength is 387 MPa and maximum elongation is 26.37%.

The mechanical properties of materials are closely related to the microstructure. The strength of Al-Zn-Mg alloys mainly comes from the strengthening of precipitates. The decrease in the density of precipitates and grain growth combined to cause a significant decrease in the tensile strength of the Al-4.5Zn-1.5Mg (wt.%) alloy after a single 350°C-FR. After the second and third straightening, the precipitates increase and produce a strengthening effect, so the tensile strength of the alloy rises and exceeds that of the

untreated alloy. As the microstructure is similar after the second and third straightening, the tensile strength values are also close to each other.

SEM images of the tensile fractures of Al-4.5Zn-1.5Mg(wt.%) alloy inside the area of flame rectification after different numbers of FR in 350°C is shown in Fig. 6. The Al-4.5Zn-1.5Mg (wt.%) alloy has relatively good plasticity. The presence of dimples of different sizes on the fracture is typical of ductile fracture. Comparing the microscopic fracture morphology in the area of untreated (Fig.6(a)) and 350°C-FR, it can be found that the dimples on the fracture after the primary rectification are smaller in size and shallower in depth relative to those in the untreated area, which indicates that the plasticity is poor. After the second straightening, the dimples become larger and deeper, and the plasticity is improved, as seen in Fig.6(c). After the third straightening, the depth of the dimples becomes shallow, and the plasticity decreases, as seen in Fig.6(d).The plastic deformation trend reflected in Fig. 6 is consistent with the mechanical performance trend in Fig. 5.

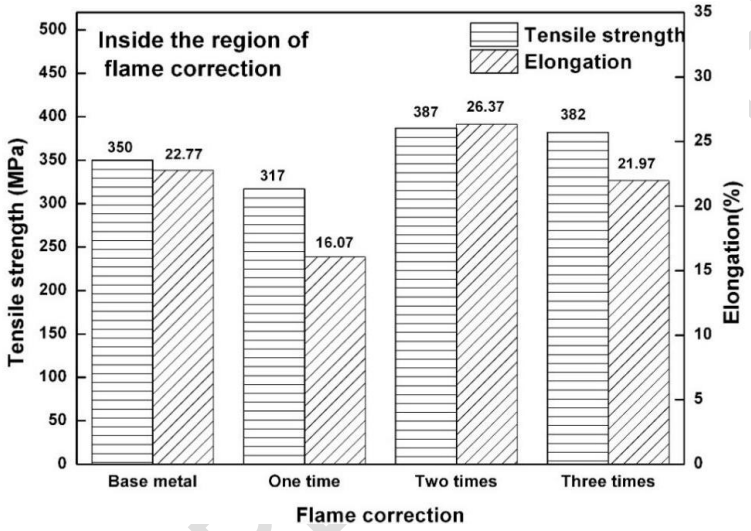

Fig. 5. Tensile strength and elongation of Al-4.5Zn-1.5Mg(wt.%) alloy inside the area of flame rectification in 350°C

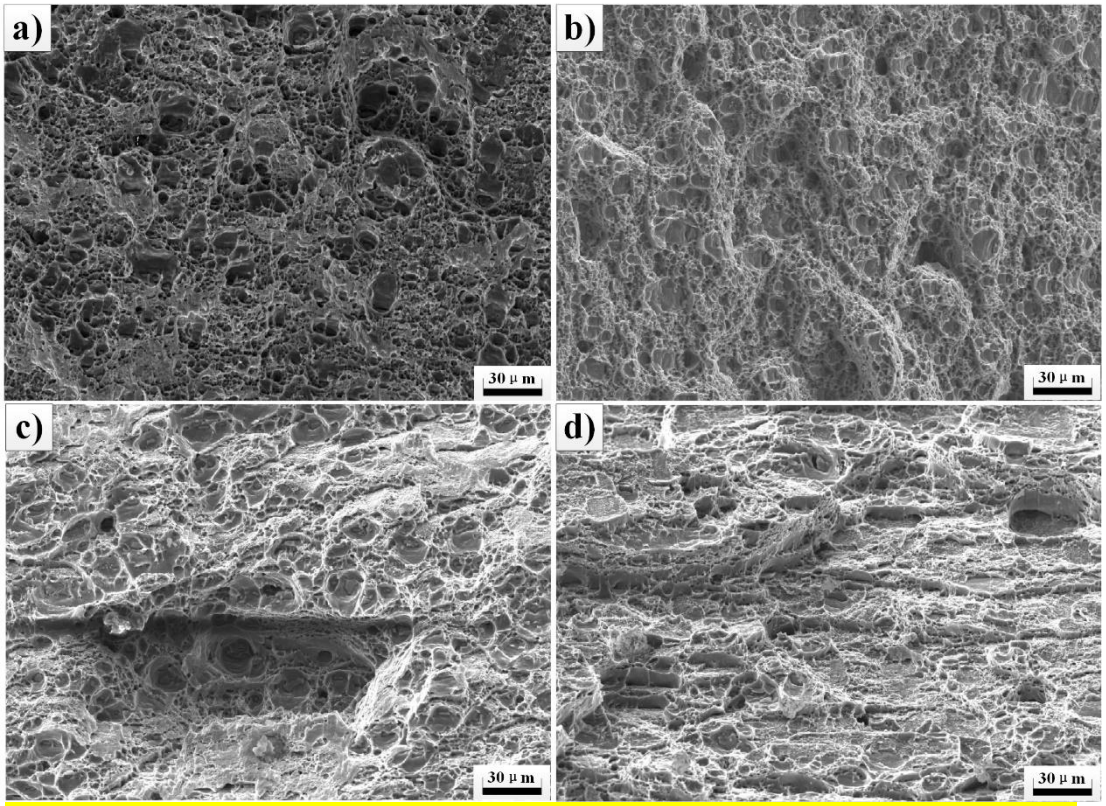


Fig. 6. SEM images of the tensile fractures of Al-4.5Zn-1.5Mg(wt.%) alloy inside the area of flame rectification after different numbers of FR in 350°C
(a) base metal, (b) one time, (c) two times, and (d) three times

The tensile strength and elongation of Al-4.5Zn-1.5Mg(wt.%) alloy outside the area of flame rectification in 350°C is shown in Fig. 7.It can be observed that the tensile strengths of the alloys outside the straightening area were all increased after FR in 350°C. This result may be related to the fact that the alloys outside the straightening area were partially recrystallized after FR in 350°C and the values of the tensile strengths did not differ much after the straightening. However, the elongation slightly increases and then decreases with increasing heating times. In addition, after the 350°C-FR, the trends of tensile strength and elongation between inside and outside the straightening area differ greatly. This is related to the heat affected zone. The inside of the straightening area is more affected by the circulating heat of the flame. The outside of the straightening area is far away from the flame, less affected by the heat, and has a slow rate of warming.

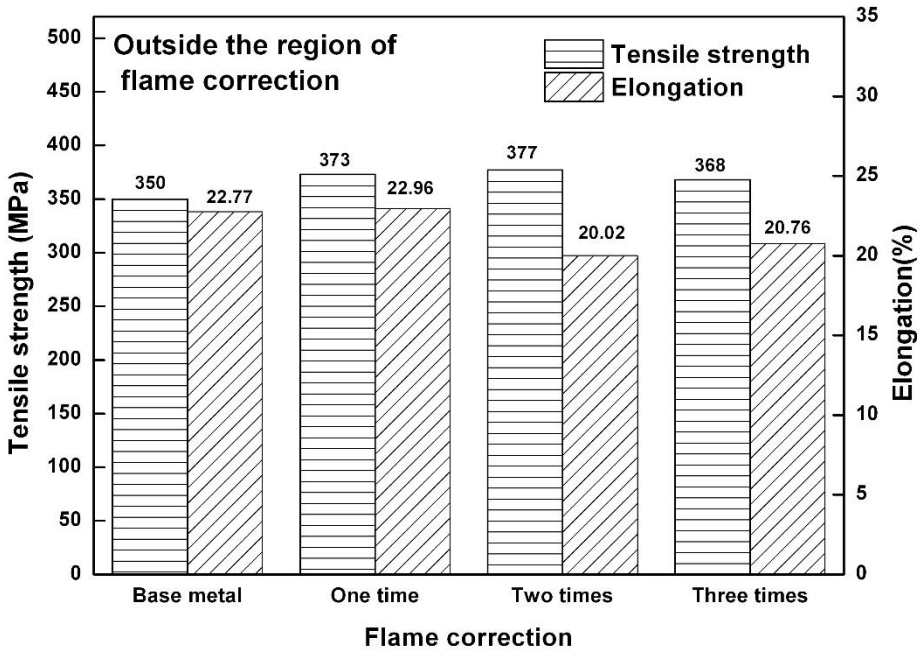


Fig. 7. Tensile strength and elongation of Al-4.5Zn-1.5Mg(wt.%) alloy outside the area of flame rectification in 350°C

TheSEM images of the tensile fractures of Al-4.5Zn-1.5Mg(wt.%) alloy outside the area of flame rectification after different numbers of FR in 350°C is shown in Fig. 8.The alloys outside the straightening area also exhibit tough fracture characteristics, and there are many dimples of different sizes on the fracture. The dimples on the fracture of unstraightened and the 350°C-FR alloys are of comparable sizes, indicating similar plasticity. After the second(Fig.8(c))and third(Fig.8(d)) straightening, the dimples decrease in size and the plasticity decreases. This trend is consistent with the extended first slight increase and then decrease in Fig. 7.

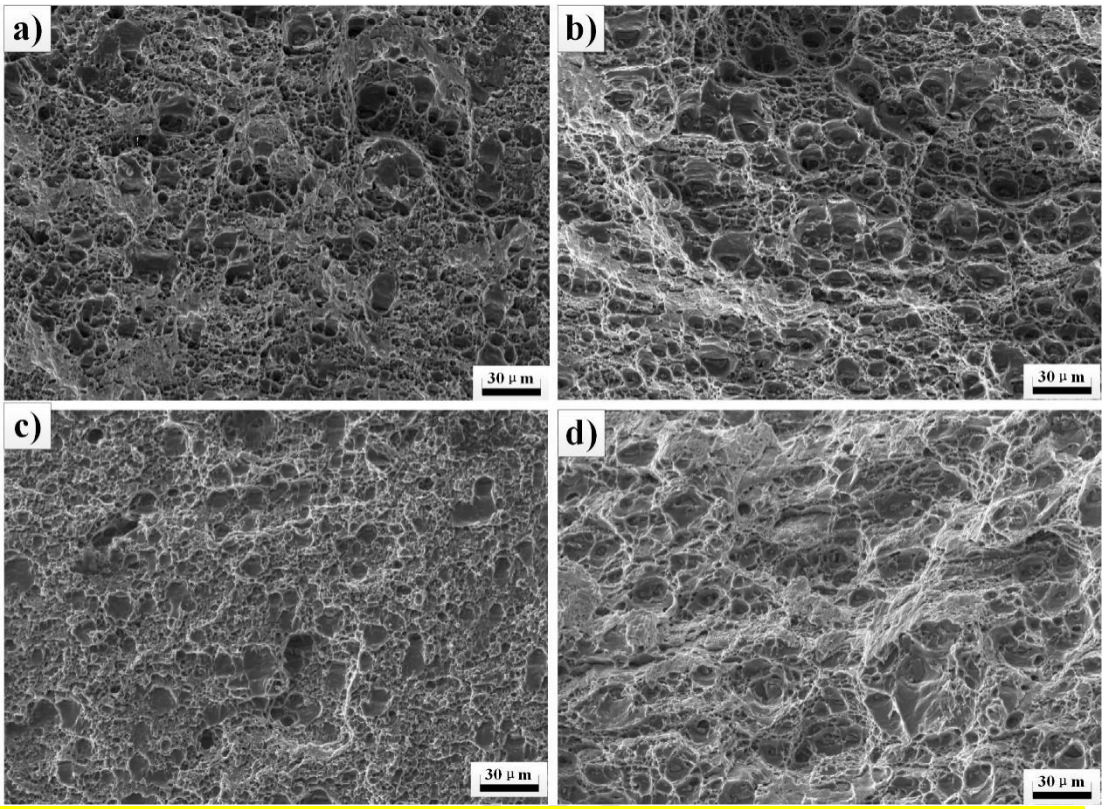

Fig. 8. SEM images of the tensile fractures of Al-4.5Zn-1.5Mg(wt.%) alloy outside the area of flame rectification after different numbers of FR in 350°C
(a) base metal, (b) one time, (c) two times, and (d) three times

### 3.3 COMPARATIVE ANALYSIS OF CORROSION PERFORMANCE

The intergranular corrosion micrographs of Al-4.5Zn-1.5Mg(wt.%) alloy inside the area of flame rectification after different numbers of FR in 350°C is shown in Fig. 9.Fig. 9 shows that after 350°C-FR, localized reticulated grain boundaries appeared in each specimen, and intergranular corrosion occurred to different degrees.Compared to others, the 350°C-FR after the first specimen corrosion is the most serious, as seen in Fig. 9(b).After the first, second and third straightening, the maximum depth of intergranular corrosion of the specimen are 0.105mm, 0.080mm, 0.076mm, and the corresponding corrosion grade are 2, 3, 3, according to GB/T7998-2005.However, intergranular corrosion is still not observed in specimens outside the straightening area. Intergranular corrosion is mainly related to the formation of primary batteries between grains and grain boundaries[16].

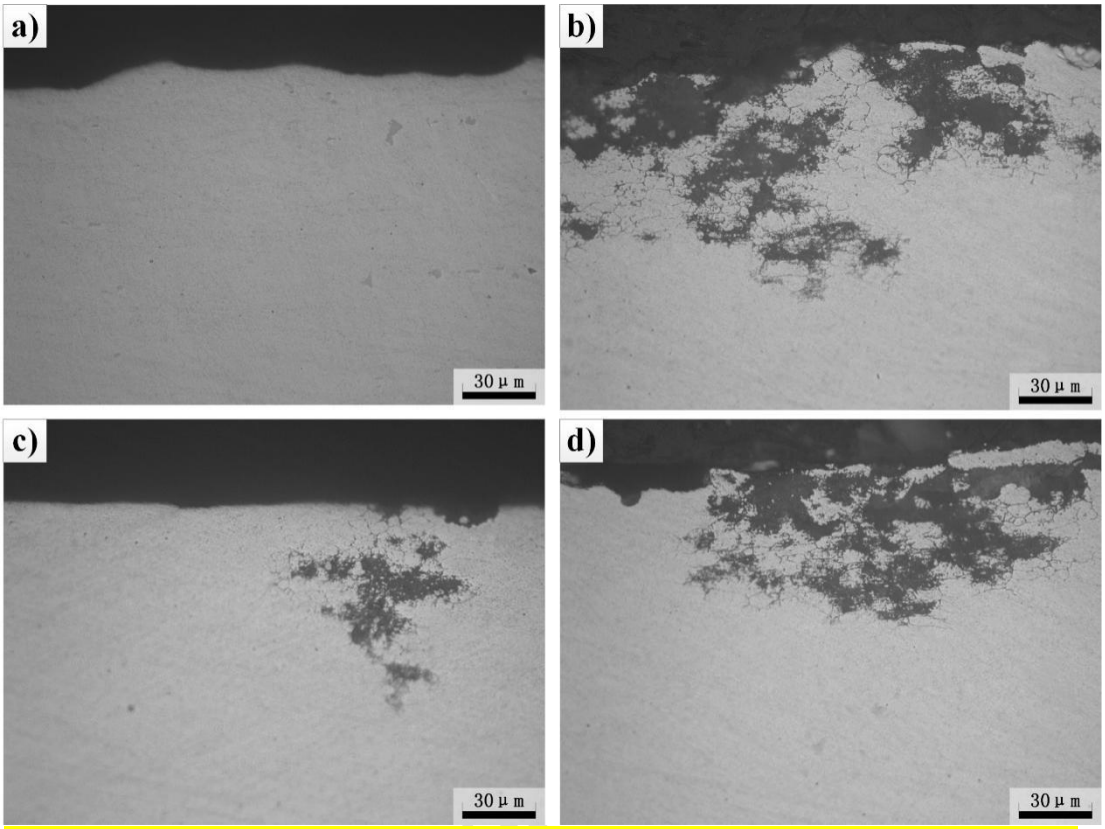


Fig. 9. Intergranular corrosion micrographs of Al-4.5Zn-1.5Mg(wt.%) alloy inside the area of flame rectification after different numbers of FR in 350°C
(a) base metal, (b) one time, (c) two times,and (d) three times

Fig. 10 shows the macroscopic morphology of exfoliation corrosion of Al-4.5Zn-1.5Mg (wt.%) alloy in the straightening area under different FR times at 350°C. It can be seen that the whole surface of the specimen in the straightening area showed uniform and severe exfoliation corrosion. The metal surface was uneven and delamination phenomenon, and the test solution after corrosion contained a large number of exfoliation products. The difference between the right side of Fig. 10(d) may be due to the sampling process is not standardized, so that the right side is taken outside the straightening area caused.

A partially exfoliated specimen was intercepted observed under the scanning electron-microscope, and the results are shown in Fig.11.Fig.11 shows that the surface of the specimen appears the crystal cracking phenomenon, and produces layer separation.Compared to others, the stripping phenomenon is the most serious in the alloy of one time FR.Fig. 11(b) shows that the specimen surface appeared obvious along the crystalline cracks, and has been deep into the metal inside quite deep. After the 350°C-FR two or three times, the corrosion degree of the specimen is not much different. Three times the specimen is slightly more serious than the second rectification specimen, along the crystal cracks slightly wider. According to GB/T22639-2008, the exfoliation corrosion level of the specimens after 350°C-FR is ED level.

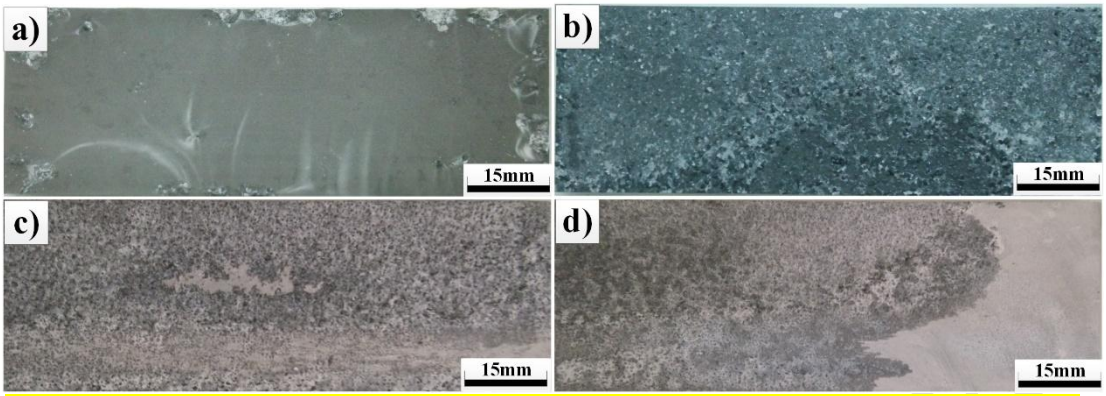


Fig. 10. Surface morphology after exfoliation corrosion of Al-4.5Zn-1.5Mg(wt.%) alloy inside the area of flame rectification after different numbers of FR in 350°C
(a) base metal, (b) one time, (c) two times, and (d) three times

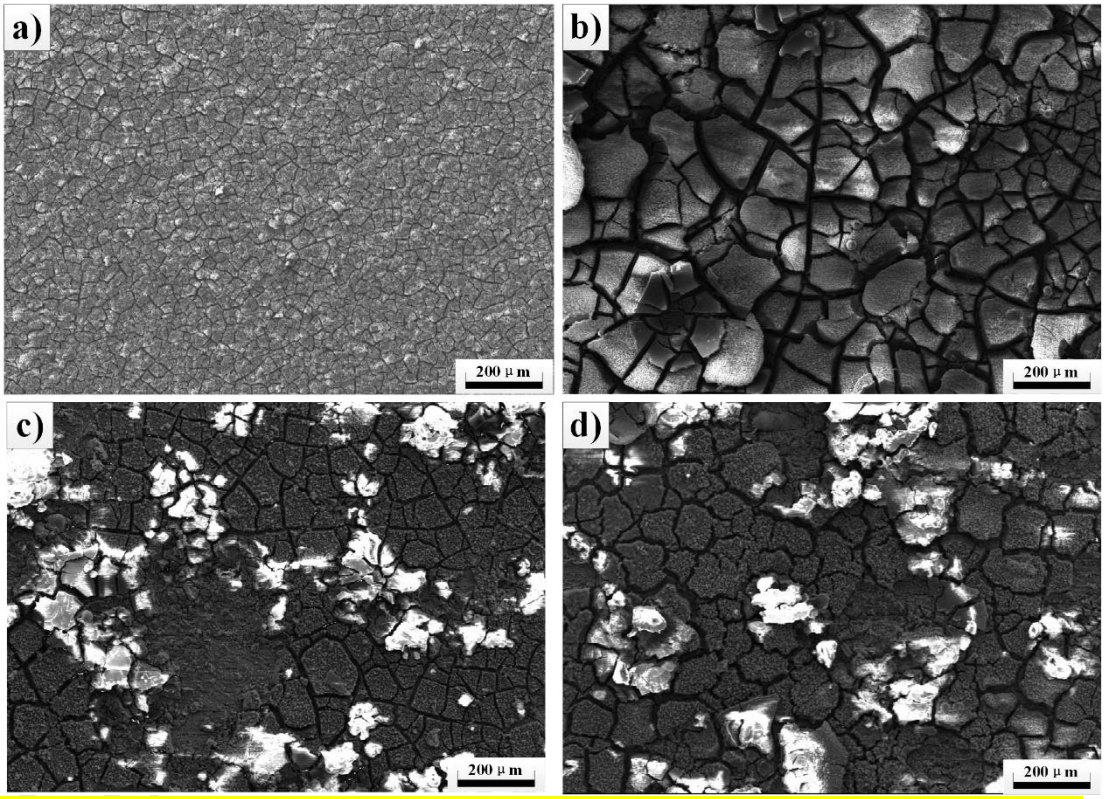


Fig. 11. SEM morphology of Al-4.5Zn-1.5Mg(wt.%) alloy after exfoliation corrosion inside the area of flame rectification after different numbers of FR in 350°C
(a) base metal, (b) one time, (c) two times, and (d) three times

The macroscopic morphology of exfoliation corrosion of Al-4.5Zn-1.5Mg (wt.%) alloy outside the straightening area at different FR times at 350°C is shown in Fig. 12. Fig. 12 shows thatthe degree of corrosion of the specimens outside the straightening area is much lighter than that inside the straightening area. The corrosion morphology of the alloy treated with FR is similar to that untreated.

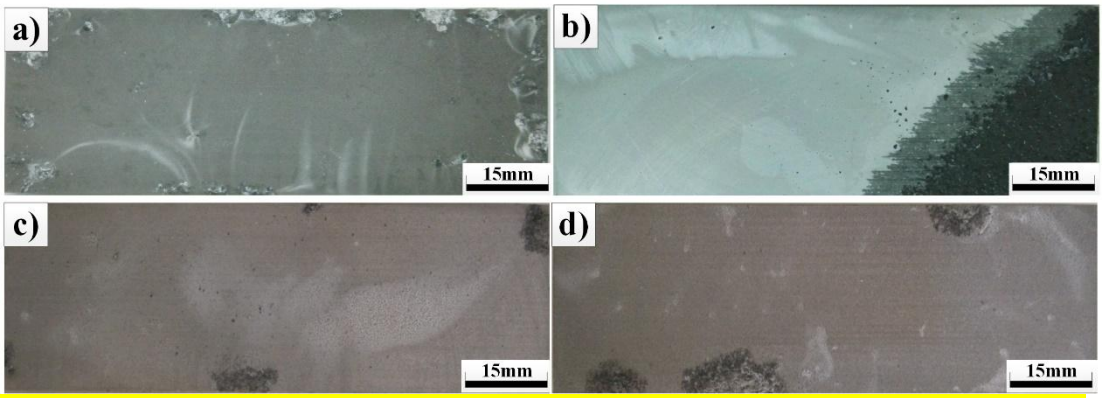

Fig. 12. Surface morphology of Al-4.5Zn-1.5Mg(wt.%) alloy after exfoliation corrosion outside the area of flame rectification after different numbers of FR in 350°C
(a) base metal, (b) one time, (c) two times, and (d) three times

Fig. 13 shows SEM morphology of Al-4.5Zn-1.5Mg(wt.%) alloy after exfoliation corrosion outside the area of flame rectification after different numbers of FR in 350°C.As can be seen from the Fig 13 (b), the exfoliation corrosion of alloy with one time 350°C-FR is the most serious.The surface appeared uniform crystalline cracks, and part of the area has appeared large pieces of metal fell off.Fig 13 (c) and (d) shows that after two times and three times FR, the specimen surface appeared uniform pits, and the corrosion pits have entered the metal surface, as seen in Fig. 14.After three times of FR, the number of corrosion products and corrosion pits in the sample was higher than that in two times of FR.According to GB/T22639-2008, the exfoliation corrosion grades of the specimens outside the 350°C-FR areas of Al-4.5Zn-1.5Mg (wt.%) alloy are EC, EB, and EB grades for the first, second, and third straightening, respectively.

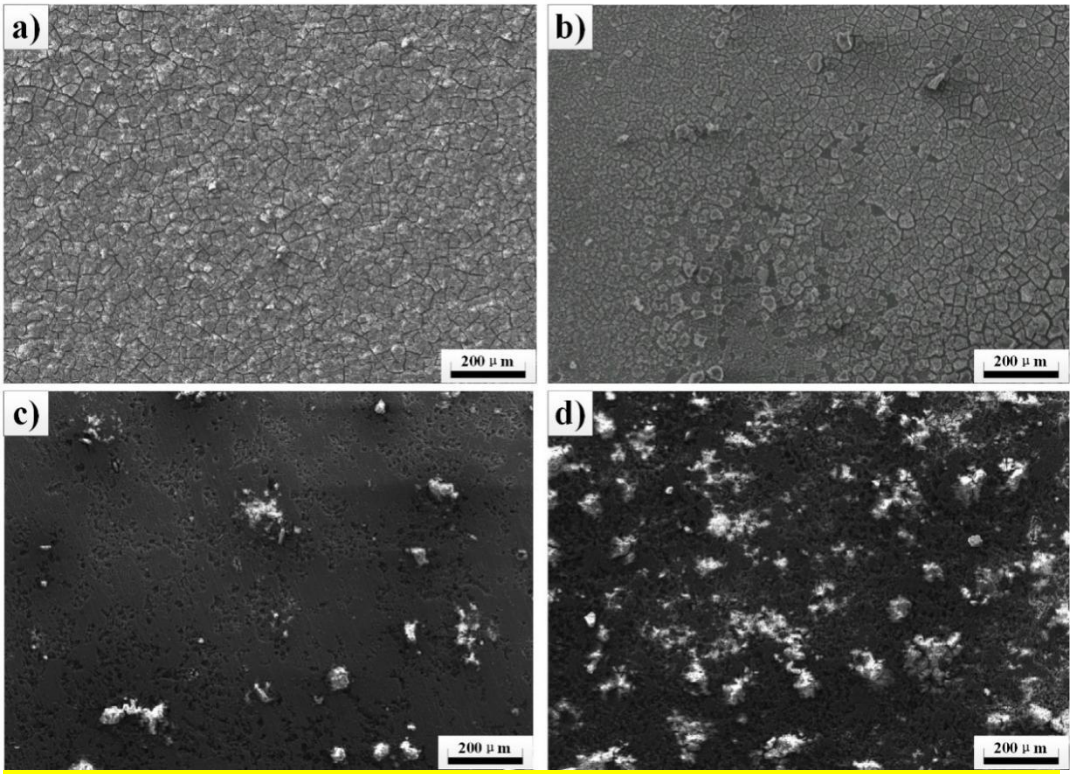

Fig. 13. SEM morphology of Al-4.5Zn-1.5Mg(wt.%) alloy after exfoliation corrosion outside

the area of flame rectification after different numbers of FR in 350°C
(a) base metal, (b) one time, (c) two times, and (d) three times

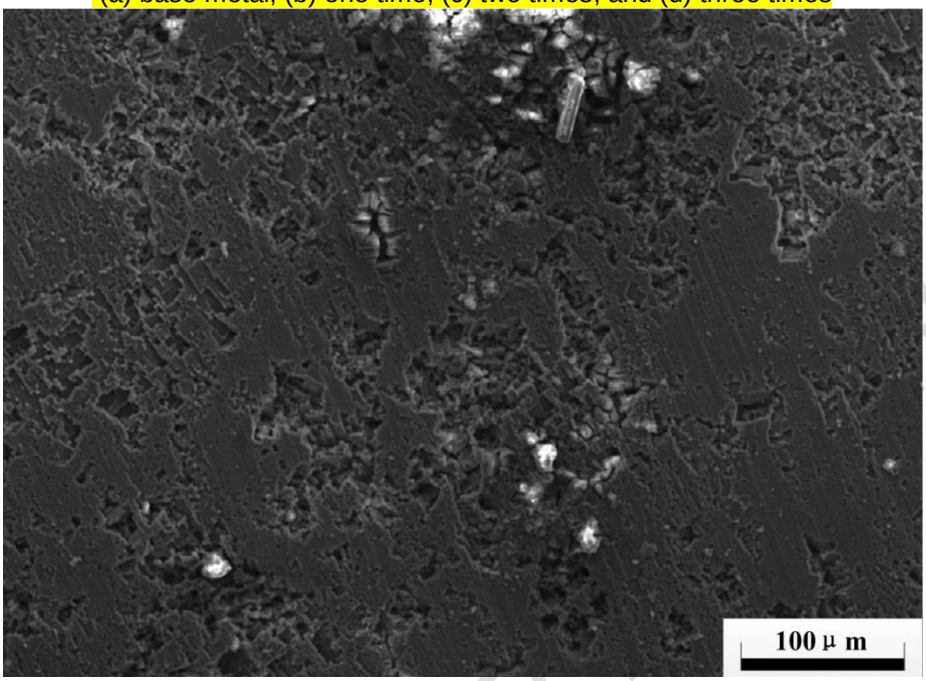


Fig. 14. Magnified morphology of Al-4.5Zn-1.5Mg(wt.%) alloy after exfoliation corrosion outside the area of flame rectification after two times of FR in 350°C

In order to analyse the reasons for the dramatic decreasingof corrosion properties in the straightening area of Al-4.5Zn-1.5Mg (wt.%) alloy withone time FR. Transmission electron microscopy was used to observe the grain boundary morphology of the specimens, and the results are shown in Figs. 15-16. From the figures, it can be seen that the precipitated phase at the grain boundaries of the Al-4.5Zn-1.5Mg (wt.%) alloy is mainly the discontinuously distributed η phase, with a size of about 100-200 nm. Fig. 15(a) shows that base metal has few precipitated phases at the grain boundaries, and their sizes were relatively large.Fig. 15(b) shows thatafter one time FR, the number of precipitated phases at the grain boundaries of the specimen increased sharply, and phases size became smaller, and the spacing decreased and tended to be continuously distributed.In addition, a non-precipitation band with a width of about 50 nm was found near the grain boundaries of the specimen after one FR at 350°C, as shown in Fig. 16.

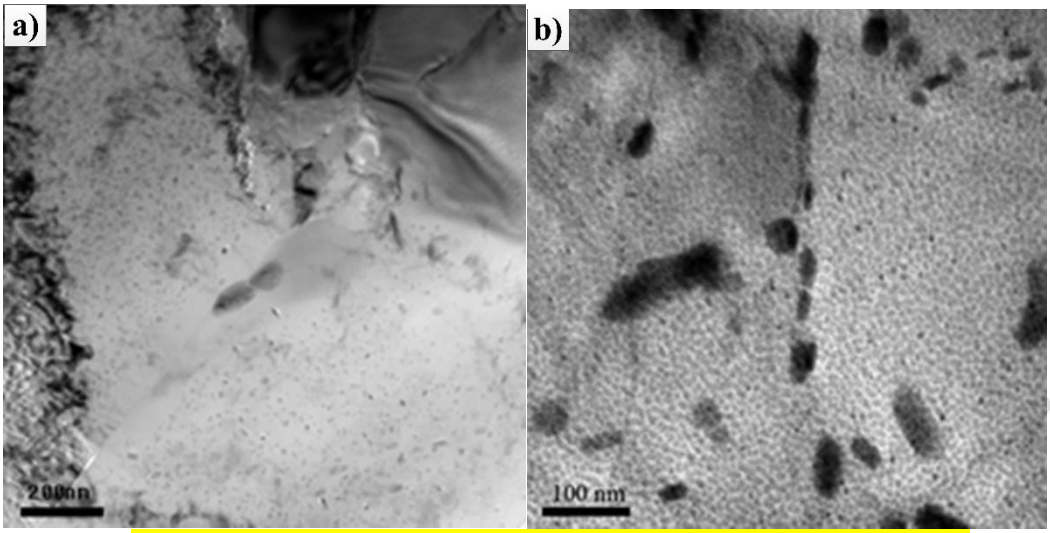


Fig. 15. TEM images of grain boundaries of Al-4.5Zn-1.5Mg(wt.%) alloy (a)base metal and (b) inside the area of flame rectification after one time of FR in 350°C

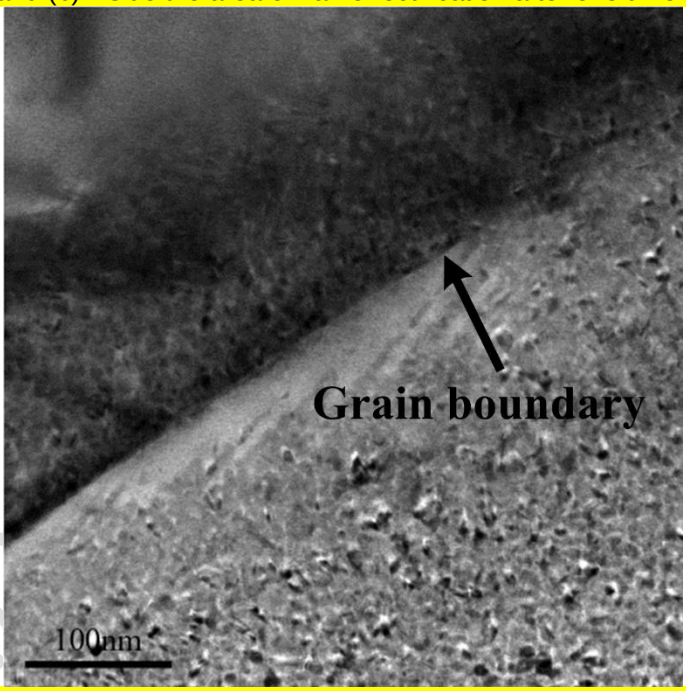


Fig. 16. TEM image of precipitation free zone of Al-4.5Zn-1.5Mg(wt.%) alloy inside the area of flame rectification after one time of FR in 350°C

The intergranular corrosion and exfoliation corrosion of Al-Zn-Mg alloys are mainly related to the formation of primary batteries.The corrosion potential of the second phase particles is high, while the potential of the base metal is low, resulting in galvanic corrosion. The base metal with low potential undergoes anodic dissolution, causing pitting corrosion. In addition, the uneven distribution of the second phase particles results in different corrosion potentials at grain boundaries and within grains, leading to galvanic corrosion. The grain boundary with low potential undergoes anodic dissolution, resulting in intergranular corrosion. With the development of intergranular corrosion, the surface metal of base metal falls off, forming exfoliation corrosion[17-21].

Therefore, the grain boundary properties of Al-Zn-Mg alloys determine their corrosion resistance. When the Al-Zn-Mg alloy without undergoing FR, the number of precipitated phases on the grain boundaries is very small, and the potential difference between the grains and the grain boundaries is small, which is not conducive to the formation of continuous corrosion channels. So, the alloy has strong resistance to intergranular corrosion.When the Al-Zn-Mg alloy undergoes one time FR, the number of precipitated phases at grain boundaries increases sharply and tends towards continuous distribution. There is a significant potential difference between the grain boundaries and the grains, which accelerates the corrosion of the alloy.

## 4. CONCLUSION

The mechanical properties and corrosion performance of Al-4.5Zn-1.5Mg(wt.%) alloy through varied flame rectifications was studied. The conclusions were drawn as follows:

(1) In the flame correction area, the mechanical properties of Al-4.5Zn-1.5Mg(wt.%) alloy with two times of flame correction is the best. The maximum tensile strength and elongation of Al-4.5Zn-1.5Mg(wt.%) alloy inside the region of flame correction are 387MPa and26.37% respectively.However, outside the flame correction zone, the mechanical properties are similar.

(2) The flame rectification accelerated the corrosion susceptibility of Al-4.5Zn-1.5Mg(wt.%) alloy. The maximum intergranular corrosion depth is detected with the value of 105μm after one time of FR.

(3)The corrosion of Al-4.5Zn-1.5Mg(wt.%) alloy is mainly related to the formation of galvanic couple.The grain boundary properties of Al-4.5Zn-1.5Mg(wt.%) alloys determine their corrosion resistance. There is a potential difference between grains and grain boundaries.

## REFERENCES


[1] TT Wang, YL Wang, X Yang et al. Cracks and process control in laser powder bed fusion of Al-Zn-Mg alloy, J. Manuf. Process.2022;81:571-579.

[2] Deng D. FEM prediction of welding residual stress and distortion in carbon steel considering phase transformation effects. Mater. Des. 2009;30:359-366.

[3] Deng D, Murakawa H. Prediction of welding distortion and residual stress in a thin plate butt-welded joint, Comp. Mater. Sci. 2008;43:353-365.

[4] Deng D, Murakawa H, Liang W. Numerical simulation of welding distortion in large structures, Comput. Method. Appl. M.2007;196:4613-4627.

[5] Zhang Z, Jiang Z, Yu C. Automated flame rectification process planning system in shipbuilding based on artificial intelligence. Int. J. Adv. Manuf. Technol. 2006;30:1119-1125.

[6] Lacalle R, Álvarez JA, Ferreño D, Portilla J,Ruiz E, Arroyo B, Gutiérrez-Solana F. Influence of the flame straightening process on microstructural, mechanical and fracture properties of S235 JR S460 ML and S690 QL structural steels, Exp.Mech. 2013;53:893-909.

[7] Shuai Li, Honggang Dong, Peng Li, Su Chen. Effect of repetitious non-isothermal heat treatment on corrosion behavior of Al-Zn-Mg alloy, Corros. Sci. 2018;131:278-289.

[8] Shuai Li, Microstructure, mechanical properties and corrosion behavior of Al-Zn-Mg alloy MIG welded joint, Dalian University of Technology, Dalian, China, 2018 D.S. Dissertation.

[9] Jiang L, Wang Y, Liu A. Effect of flame straightening on microstructures and properties of welded joint of aluminium alloy for high-speed train, T Mater. Heat Treat. 2003;24:59-61.

[10] Xiong Z. Effect mechanism of heat-straightening temperature on microstructure and properties of Aluminum alloy joint in high-speed trains. Harbin Institute of Technology, Harbin, China. M.S. Dissertation; 2014.

[11] Avent RR. Heat-straightening of steel –Fact and fable, J. Struct. Eng. ASCE.1989;115:2773-2793.

[12] Avent RR, Fadous GM. Heat-straightening prototype damaged bridge girders, J. Struct. Eng. ASCE. 1989; 115:1631- 1649.
[13] Avent RR, Mukai DJ. What you should know about heat straightening repair of damaged steel. Eng. J. AISC. 2001; 38:27-49.
[14] ASTM G110-92. Standard practice forevaluatingintergranular corrosion resistance of heattreatable aluminum alloys by Immersion in Sodiumchloride + hydrogen peroxide solution; 2009.
[15] ASTM G34-01. Standard test method for exfoliation corrosion susceptibility in 2xxx and 7xxx Series Aluminum Alloys (EXCO Test); 2013.
[16] P Li, YQ Wang, S Wang et al. Corrosion behavior of refiled friction stir spot welded joint between aluminium alloy and galvanized steel, Mater Res Express. 2018; 5:096524.
[17] QY Ding, YX Qin, YY Cui. Galvanic corrosion of aircraft components in atmospheric environment, J. Chin. Soc. Corrosi. Protect, 2020; 40(5):455–462
[18] YT Ma, HG Dong, YQ Wang et al. Effect of Zn coating on microstructure and corrosion behavior of dissimilar joints between aluminum alloy and steel by refiled friction stir spot welding, J. Appl. Electrochem, 2022;52:85-102.
[19] J Kang, R Fu, G Luan, et al. In-situ investigation on the pitting corrosion behavior of friction stir weldedjoint of AA2024-T3 aluminium alloy, Corros. Sci., 2010; 52:620-626.
[20] R Ly, KT Hartwig, H Castaneda. Effects of strain localization on the corrosion behavior of ultra-finegrained aluminium alloy AA6061,Corros. Sci. 2018; 139:47-57.
[21] P Li, YQ Wang, S Wang, et al.Corrosion behavior of refilled friction stir spot welded joint between aluminum alloy andgalvanized steel, Mater. Res. Express.2018; 5(9):096524.